

# Thermo-Acoustic Simulation of a Piezoelectric Transducer for Interstitial Thermal Ablation with MRTI Based Validation

K. Y. Gandomi<sup>1</sup>, P. A. Carvalho<sup>1</sup>, Z. Zhao<sup>1</sup>, C. J. Nycz<sup>1</sup>, E. C. Burdette<sup>2</sup>, and G. S. Fischer<sup>1</sup>

<sup>1</sup>Robotics Engineering, Worcester Polytechnic Institute, Worcester, MA, United States

<sup>2</sup>Acoustic Medsystems Inc, Savoy, IL, United States

## Abstract

The primary aim of cancer treatment is to remove malignant cells while conserving parenchymal tissue. Achieving appropriate margins can be difficult for deep brain tumors that are unsuited for conventional surgical interventions. One minimally invasive treatment option under research for these clinical cases is needle based therapeutic ultrasound (NBTU). The NBTU probe consists of a cylindrical piezoelectric transducer which, when excited, produces high frequency acoustic waves that are absorbed by the tumor leading to localized heating and death of cancer cells. In order to effectively ablate the entire area of the tumor and minimize damage to healthy cells, model-based control of thermal dose may be necessary. In this work, we present a thermo-acoustic multi-physics COMSOL simulation of a two dimensional NBTU probe and validate the model using magnetic resonance thermal imaging (MRTI).

## Introduction

The five year survival rate for malignant brain and central nervous system cancer was estimated at 35% between 2000 and 2015 [1]. Achieving appropriate margins when surgically treating complex shaped tumors is vital for reducing remission [2]. This can be particularly challenging in delicate tissues such as the brain. Treatment options that closely trace asymmetric tumor boundaries can conserve healthy tissue while removing cancerous cells.

Interstitial NBTU for conformal tumor ablation has been studied in recent years for these clinical cases [3–5]. A small burr hole is made through which a cylindrical sectored piezoelectric transducer is inserted to the tumor site. Heating from the directed ultrasound waves produced by the transducer can be used to ablate a desired shape [6, 7]. Monitoring of the heat propagation from the NBTU in real-time is possible with MRTI [8].

MRI compatible surgical robots have been demonstrated [9] which allow for precise placement of an NBTU probe in the brain. An ablation control system using thermal propagation modeling paired with a robot's precision and under closed-loop from MRTI feedback may increase ablation accuracy. In this paper, we develop and experimentally validate a thermal model of the NBTU probe in a homogeneous medium using COMSOL 5.3a in two dimensions (2D), as a step towards incorporating such

models into closed-loop control of the ablation boundary.

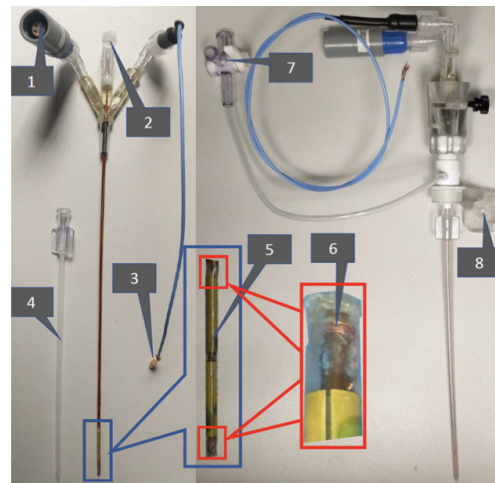


**Figure 1.** MRI Compatible NBTU probe used for interstitial thermal ablation developed by Acoustic Systems Inc. with labeled components: (1) Connector for the ablation element (2) Cooling water inlet (3) Connector for tracking coil interface (4) Outer sleeve for water (5) High intensity ultrasound ablation elements (6) Micro tracking coils (7) Outlet for water (8) Fixture for attaching the probe

## Operating Principle

The inverse piezoelectric effect refers to the capability of certain materials to strain when subject to an electric potential. Piezoelectric ultrasonic transducers make use of this property to rapidly oscillate under an applied alternating field to produce acoustic waves. These waves, when absorbed by the surrounding medium, cause heating. The change in temperature depends on both the properties of the transducer and medium.

The transducer geometry and material determines the ideal driving excitation frequency (resonance) as well as produced wave properties such as beam shape, directionality, and amplitude. The applied electric potential to the transducer drives the deformation and contributes to the overall energy deposition of the produced acoustic waves. Lead zirconium titanate (PZT) is a material that exhibits the inverse piezoelectric effect and is commonly used when designing ultrasonic transducers.

The medium properties control how well these waves are transmitted within the material. Acoustic attenuation

refers to the decrease in wave amplitude as a function of distance traveled within the specified material. A large attenuation coefficient signifies waves are quickly absorbed. Thermal conductivity of the medium, the rate of heat transfer, and heat capacity of the medium, the energy required to produce a temperature change, also contribute to the observed heating induced by the transducer.

### NBTU Model Setup

The NBTU probe developed by Acoustic Medsystems Inc (Illinois, United States) is shown in Figure 1. A 2D COMSOL component was used to build, in simulation, a cross-sectional slice perpendicular to the probe axis using the COMSOL geometry tools. A difference between two concentric circles (1.1mm inner diameter x 1.5mm outer diameter) was used to create the initial probe body. Four notches (0.1mm depth x 0.05mm width) were added such that the probe was segmented into 90° and 180° sectors as shown in figure 2 using the difference operator. Electrically exciting a given sector between a pair of notches can produce a 90° or 180° acoustic beam respectively. Lead zirconate titanate (PZT-4) from the COMSOL material library was selected as the probe material with no modifications.

The probe body was centered within a 100mm x 100mm homogeneous square that represented the acoustic phantom medium. A COMSOL *blank* material was imported with custom properties based on those measured in [10] consisting of a heat capacity at constant pressure of 3451 J/(Kg \* K), thermal conductivity of 0.53 W/(m \* K), density of 1058 Kg/m<sup>3</sup>, and speed of sound within the material of 1551 m/s. The inner circle of the probe in the simulation was also defined with this material since the mechanical properties of this region should have little influence over the modeled results.

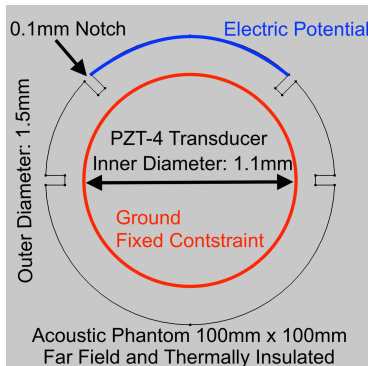


**Figure 2.** COMSOL probe simulation setup based on axially perpendicular cross-section of a transducer. Blue curve represents the 90° sector that is excited in the simulations.

Two pairs of tetrahedral meshes were created: One for the acoustic pressure field frequency domain study

and one for the thermal propagation time domain study. These studies are explained in upcoming sections of this paper. For both studies, COMSOL’s default *fine* mesh was used for the transducer and its inner circle area. For the medium in the frequency domain study, a mesh with maximum element size of  $\lambda/6$  was used to allow for an accurate representation of the pressure gradients, where  $\lambda$  represents the wavelength of the produced acoustic waves. For the medium in the time domain study, the default *extremely fine* mesh was used to allow for faster computation without degrading result quality.

### Physics Module Setup

The acoustic-piezoelectric interaction - frequency domain multi-physics module was imported, bringing in the solid mechanics, electrostatics, and pressure acoustic physics interfaces.

The solid mechanics interface was applied only to the transducer. The probe was defined as a piezoelectric material and the inner circumference of the transducer was given a fixed constraint. A base vector coordinate system was created facing radially outward from the center of the transducer to define the poling direction of the piezoelectric element. This is accomplished by creating a transformation from the local coordinate frame (x1, x2, x3) into a cylindrical frame. Table 1 shows the resulting equations where (X, Y) refers to the material coordinate system and (x,y) refers to the spatial coordinate system.

Base Vectors	x	y
x1	$-\sin(\text{atan2}(Y,X))$	$\cos(\text{atan2}(Y,X))$
x3	$\cos(\text{atan2}(Y,X))$	$\sin(\text{atan2}(Y,X))$

**Table 1.** Base vector coordinate frame used to give the poling direction of the piezoelectric element.

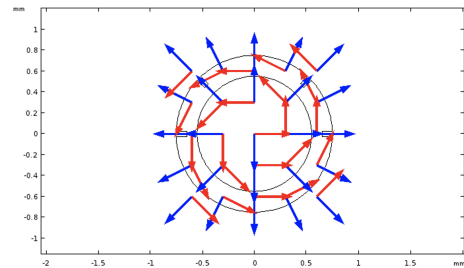


**Figure 3.** The base vector coordinate frame for element poling plotted on the transducer in COMSOL.

The electrostatics interface was also applied to the transducer. An electric potential of 7.8V was applied to the 90° notched segment of the probe as shown by blue curve in figure 2. This voltage was selected experimentally. The inner circumference of the transducer was defined as ground (red curve in figure 2).

The pressure acoustic interface was applied only to the acoustic phantom medium using the reference pressure for water and defining a typical wave speed for perfectly matched layers as 1483 m/s. The fluid model was set as “linear elastic with attenuation” where the speed of sound and density are imported from the material and the attenuation coefficient was set to 31.96 Np/m. A far-field and cylindrical radiation condition were applied to the external medium perimeter. The equation used within the pressure acoustic physics module was set to the frequency domain study used for the acoustic field calculation.

The bioheat transfer interface was also imported into the simulation and applied only to the acoustic phantom medium. The boundary of the medium was defined as thermally insulated. A heat source was created over the domain with a user defined function as shown in equation 1 where  $Q$  is the absorbed ultrasound energy over the acoustic field,  $acpr.Q_{pw}$  is the dissipated power intensity,  $step$  is a COMSOL step function from 0 to 1 with smoothing of 0.005,  $t$  is the current time step of the simulation, and  $t_{probeOn}$  is a constant that represents the total time the transducer should be activated. The resulting heat source,  $Q$  is used within the Pennes’ Bioheat Transfer equation to model energy transfer from the transducer. Tissue properties are assumed not to change as the simulation progresses and blood perfusion is not considered.

$$Q = acpr.Q_{pw} * step(t - t_{probeOn}) \quad (1)$$

### Determining Resonant Frequency

The resonant frequency, or natural frequency, of a piezoelectric transducer is largely dependent on the geometry and material of construction. At the resonant frequency the amplitude of probe deformation is at a relative maximum. To determine these key frequencies for the designed transducer, a COMSOL boundary probe was placed on the outer circumference of the two dimensional model to measure total displacement,  $solid.disp$ . A frequency domain study was used to sweep from 1 MHz to 10 MHz at 0.1 kHz steps to find those frequencies with the highest transducer deformation since the physical probes tend to operate within this range. This study only used the solid mechanics and electrostatics physics interfaces. The results of the study are shown in figure 4. Each peak was then qualitatively evaluated for beam pattern and acoustic intensity. The resulting selected resonant mode was 5.237 MHz.

### Computing Acoustic Pressure Field

The acoustic pressure field is a required component for deriving acoustic intensity and for calculating thermal propagation by the modeled transducer. A second frequency domain study conducted at the resonant frequency

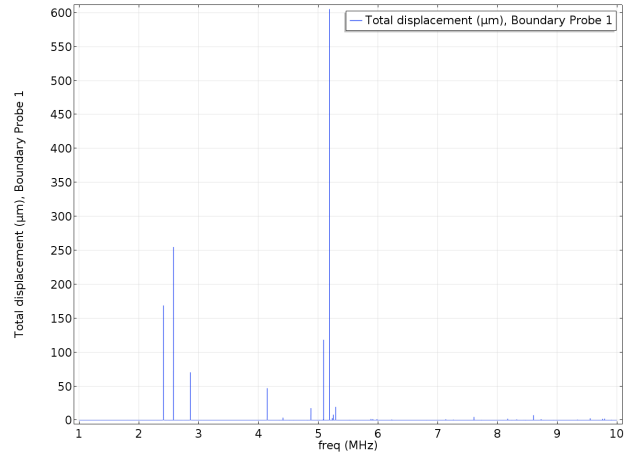


**Figure 4.** Total solid displacement measured by boundary probe (um) vs. frequency (MHz). The frequency sweep ranges from 1 MHz to 10 MHz at 0.1 kHz steps.

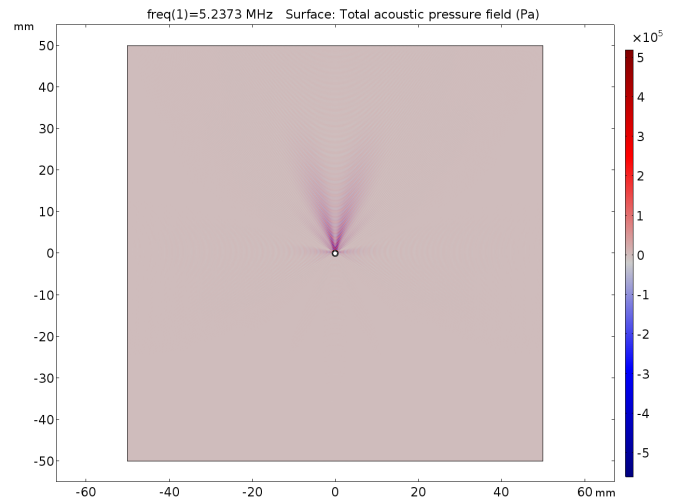


**Figure 5.** Calculated acoustic pressure map from frequency domain study at resonant frequency of 5.237 MHz.

was created using the pressure acoustics, solid mechanics, and electrostatics physics interfaces. The resulting acoustic pressure field is shown in figure 5 and depicts a 90° ultrasonic beam pattern that attenuates with distance from the source. This result agrees well with the physical probe specifications.

### Computing Heat Propagation

A time domain study was conducted to simulate medium heating due to the acoustic energy produced by the modeled transducer. The study exclusively used the bioheat transfer physics interface and relied on the previously calculated acoustic pressure field study as a dependent variable. The study was conducted over 480 seconds with 3 second time steps. The transducer was enabled during the first 240 seconds producing heating in the medium and

disabled during the second 240 seconds to allow for cooling via conduction. Surface plots of simulated medium temperature after 60, 120, and 240 seconds of insonation are depicted in figures 7(a), 7(c), and 7(e) respectively. The maximum observed temperature was  $26.7^{\circ}\text{C}$ .

### Experimental Validation

The heat propagation computed in the COMSOL time domain study was validated experimentally by monitoring an ablation under MRTI with the physical NBTU probe. A phantom built using the recipe in [10] and whose acoustic properties were modeled in simulation was used as the experimental medium. The NBTU probe was setup in the phantom as shown in figure 6 and placed within the bore of an Achieva 3T MRI scanner (Philips, USA). Two flex coils were placed on either side of the phantom for imaging. Scans were taken perpendicular to the probe axis and centered at the piezoelectric element. An echo planner fast field echo (FFE-EPI) scan at  $1.5\text{mm} \times 1.5\text{mm} \times 4\text{mm}$  voxels was used. The NBTU probe was turned ON using the Theravision software (Acoustic Medsystems Inc, Illinois, United States) with a driving frequency of about 7 MHz. Ablation was conducted for 240 seconds followed by 240 seconds of cooling. Note that the excitation frequency of the probe used in the experiments was different from the simulation. This may be related to differences caused by specific probe construction.

A comparison between the developed COMSOL simulation and MRTI images are shown side by side for select time steps in Figure 7. A vertical line crossing through  $x = 0$  for the simulated and measured temperature maps at  $t = 240\text{s}$  is shown in figures 8(a) and 8(b). The corresponding thermal readings along this line are plotted in figure 8(c). Through this vertical line the computed RMS error between the simulated and experimental temperatures was  $0.53^{\circ}\text{C}$  with a maximum computed difference of  $1.54^{\circ}\text{C}$ .

### Conclusion

A multiphysics simulation of a piezoelectric transducer used for interstitial NBTU brain tumor ablation was presented. Frequency domain and time domain studies were conducted for acoustic pressure field and thermal heating calculation respectively. The resulting thermal-propagation simulation was compared with experimental probe performance measured by MRTI showing a worst case error of  $1.54^{\circ}\text{C}$  taken along a vertical line through the center of the transducer heating field. Future work will focus on exploring 3D modeling of ablation patterns created by these transducers as well as developing dynamic models of rotating probes for closed loop control schemes to be used by surgical robot systems. Non-static material properties and perfusion will also be explored in future

models.

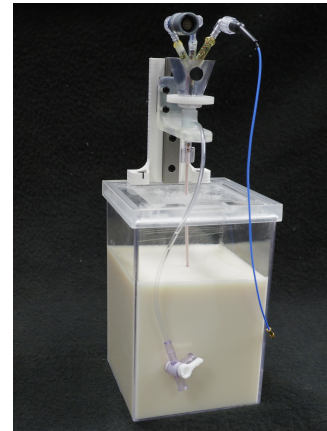


**Figure 6.** NBTU probe within phantom of known acoustic properties prior to placement within the MRI and thermal ablation with MRTI data collection.

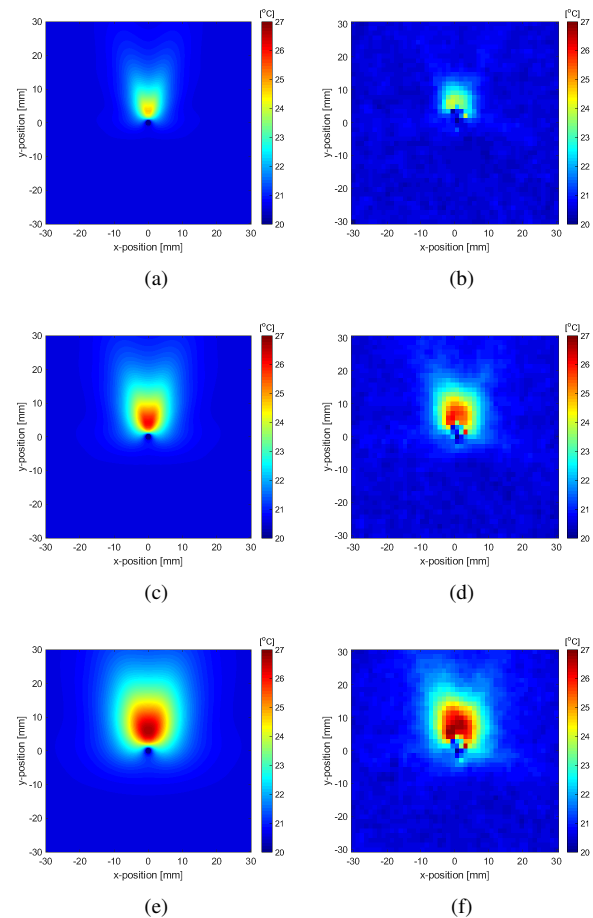


**Figure 7.** Thermal map comparison between COMSOL Simulation (left) and collected MRTI data (right) at timesteps (a/d) 60s (b/e) 120s (c/f) 240s



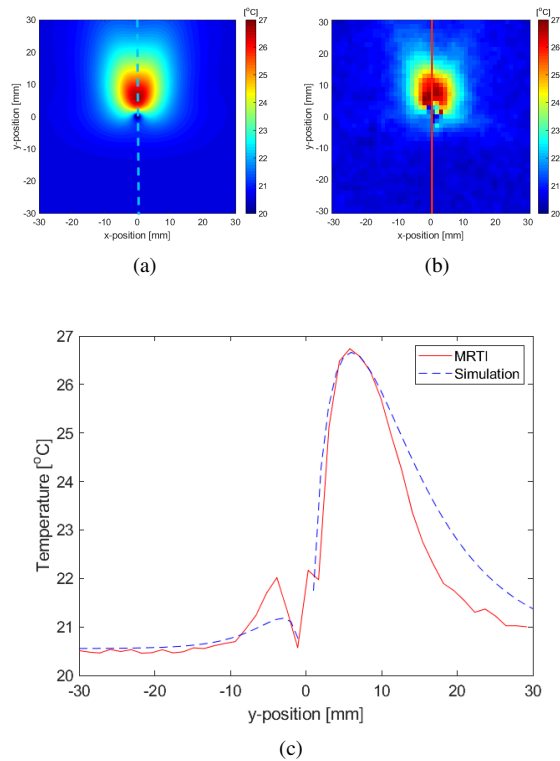


**Figure 8.** In (c), a comparison between simulated versus measured temperature readings along  $y$  at  $x = 0$  for  $t = 240s$  as shown in (a/b). The break in the plot in (c) represents the probe center.

## Funding Data

- National Institutes of Health (NIH) under the National Cancer Insituton (NCI) (Grant No. R01 CA166379)

## References

1. Ostrom, Q. T. *et al.* CBTRUS Statistical Report: Primary Brain and Other Central Nervous System Tumors Diagnosed in the United States in 2011–2015. *Neuro-Oncology* **20**, iv1–iv86, DOI: 10.1093/neuonc/noy131 (2018). [http://oup.prod.sis.lan/neuro-oncology/article-pdf/20/suppl\\_4/iv1/26608165/noy131.pdf](http://oup.prod.sis.lan/neuro-oncology/article-pdf/20/suppl_4/iv1/26608165/noy131.pdf).
2. Lacroix, M. *et al.* A multivariate analysis of 416 patients with glioblastoma multiforme: prognosis, extent of resection, and survival. *J. neurosurgery* **95**, 190–198 (2001).
3. Diederich, C. J., Nau, W. H. & Stauffer, P. R. Ultrasound applicators for interstitial thermal coagulation. *IEEE transactions on ultrasonics, ferroelectrics, frequency control* **46**, 1218–1228 (1999).

4. Scott, S. J., Salgaonkar, V., Prakash, P., Burdette, E. C. & Diederich, C. J. Interstitial ultrasound ablation of vertebral and paraspinal tumours: Parametric and patient-specific simulations. *Int. J. Hyperth.* **30**, 228–244 (2014).
5. Lafon, C., Melodelima, D., Salomir, R. & Chapelon, J. Y. Interstitial devices for minimally invasive thermal ablation by high-intensity ultrasound. *Int. J. Hyperth.* **23**, 153–163 (2007).
6. Burdette, E. C. *et al.* Conformal needle-based ultrasound ablation using em-tracked conebeam ct image guidance. In *Energy-based Treatment of Tissue and Assessment VI*, vol. 7901, 790107 (International Society for Optics and Photonics, 2011).
7. Chopra, R., Luginbuhl, C., Foster, F. S. & Bronskill, M. J. Multifrequency ultrasound transducers for conformal interstitial thermal therapy. *IEEE transactions on ultrasonics, ferroelectrics, frequency control* **50**, 881–889 (2003).
8. Quesson, B., de Zwart, J. A. & Moonen, C. T. Magnetic resonance temperature imaging for guidance of thermotherapy. *J. Magn. Reson. Imaging: An Off. J. Int. Soc. for Magn. Reson. Medicine* **12**, 525–533 (2000).
9. Nycz, C. J. *et al.* Mechanical validation of an mri compatible stereotactic neurosurgery robot in preparation for pre-clinical trials. In *2017 IEEE/RSJ International Conference on Intelligent Robots and Systems (IROS)*, 1677–1684 (IEEE, 2017).
10. Farrer, A. I. *et al.* Characterization and evaluation of tissue-mimicking gelatin phantoms for use with mrgfus. *J. therapeutic ultrasound* **3**, 9 (2015).